Supplementary Material - Active nematic coherence probed under spatial patterns of distributed activity

Ignasi Vélez-Cerón,[1,2] Jordi Ignés-Mullol,[1,2] and Francesc Sagués[1,2]

[1] *Department of Materials Science and Physical Chemistry, Universitat de Barcelona, 08028 Barcelona, Spain*
[2] *Institute of Nanoscience and Nanotechnology, IN2UB, Universitat de Barcelona, 08028 Barcelona, Spain*

(Dated: September 28, 2024)

I. SUPPLEMENTARY FIGURES

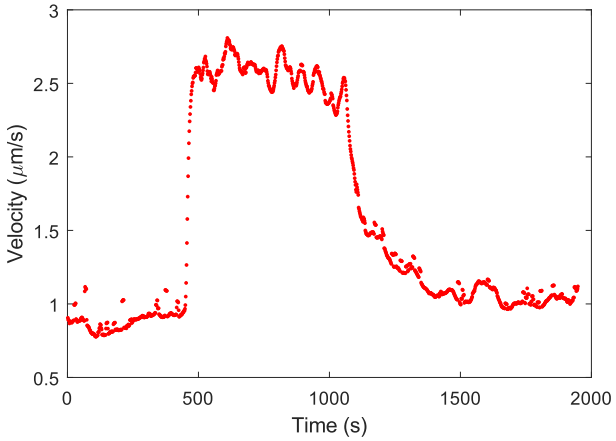

FIG. S1. **Speed contrast contrast.** a) Average speed in a photosensitive active nematic layer. Light is activated at 450 s, and deactivated at 1050 s. The irradiation light power density in the ON state is *c.a.* 17 mW cm^{-2}.

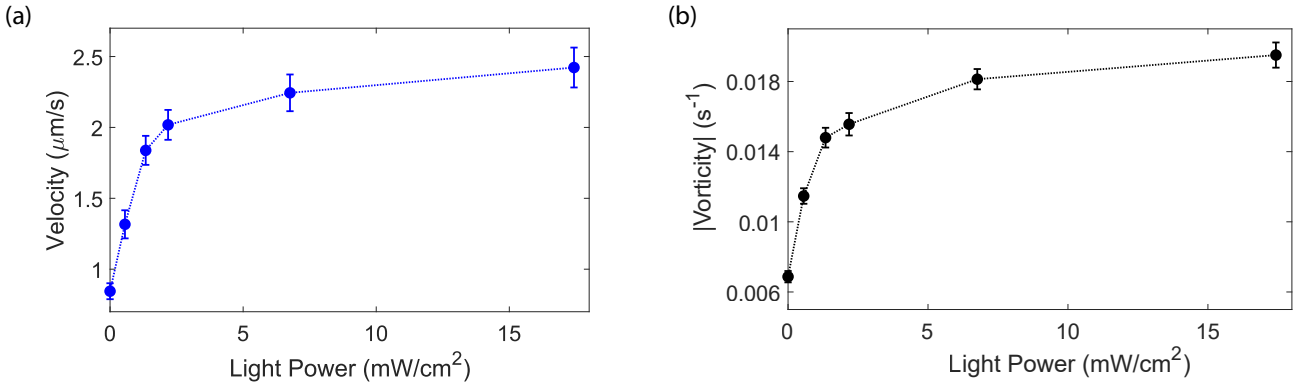

FIG. S2. **Effect of power density.** a) Average steady-state speed in a photosensitive active nematic layer for different power densities of illumination. Data corresponds to the spatial and temporal average of three independent experiments in each case. b) Average steady-state vorticity for the same experiments. Error bars are the standard deviation of the mean. Their relative value in the velocity data is roughly twice that of the vorticity data.

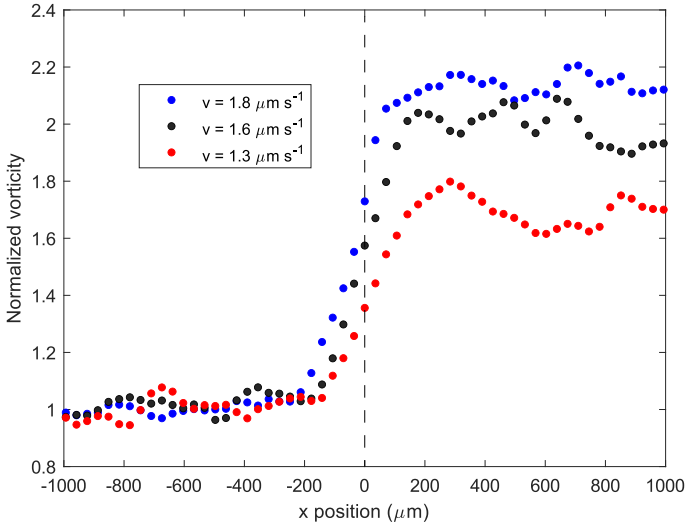

FIG. S3. **Thickness of the penetration depth.** Average vorticity profile along a region that is half illuminated (right) and half dark (left), for different activities (quantified here with the average speed of the illuminated region). The measured penetration depths of light excitation into the dark region for these three experiments are 159 ± 22 μm (●), 176 ± 22 μm (●), and 219 ± 20 μm (●). By multiplying the average speed in the illuminated region (inset) by $t_{OFF} \simeq 2$ min, we obtain an estimation for the transition region of 156 ± 15 μm, 192 ± 17 μm, and 216 ± 23 μm, respectively. Once we take into account the uncertainty in the average speed and that in the value of t_{OFF}, these estimations agree with the measure values reported above.

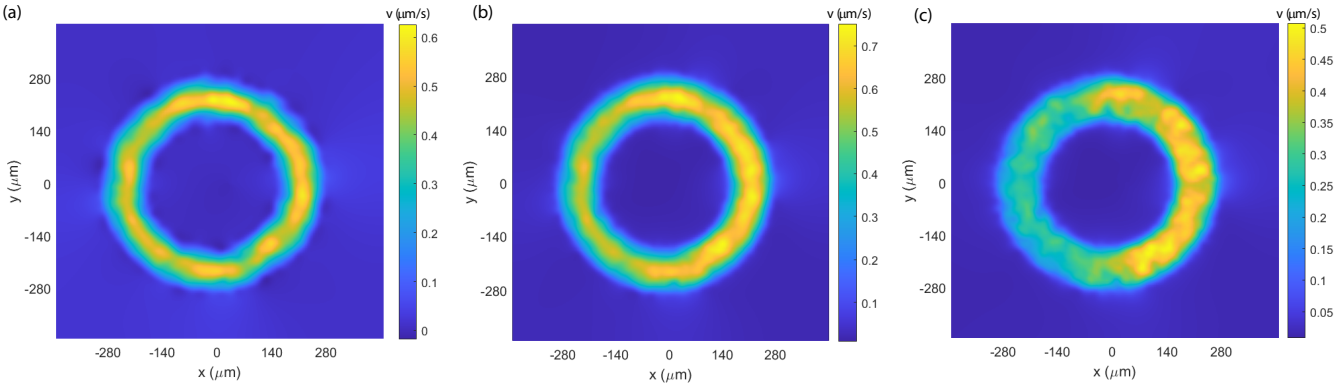

FIG. S4. **Speed contrast in half-illuminated ring.** Colormap illustrating the time-averaged velocity in an AN confined inside a ring-shaped channel of width 140 μm. The right half of the ring is illuminated, while the left half remains in the dark. (a) Azimuthal component of the velocity. (b) Speed. (c) Radial component of the velocity (absolute value).

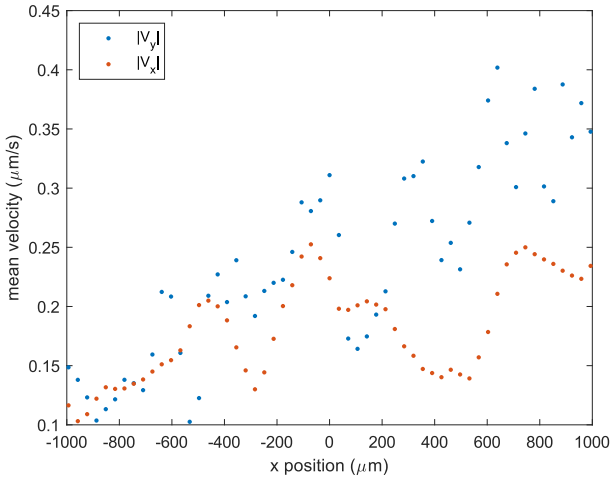

FIG. S5. **Alignment transition.** Average steady-state velocity components in an active nematic layer with 10% the normal activity, prepared in contact with an anisotropic oil. The region to the left of x = 0 is in the dark, while the region to the right of x = 0 is illuminated.

II. SUPPLEMENTARY MOVIES

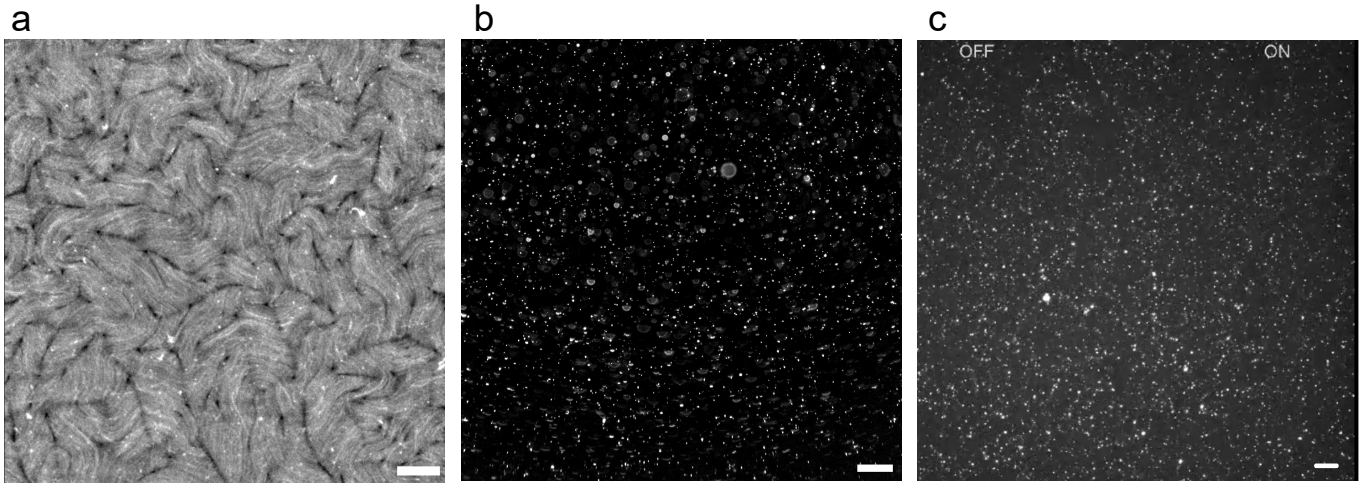

Movie S1. **Photosensitive active nematic.** (a) Fluorescence images. In the first part, the whole field of view is illuminated. In the second part, only parts of the field of view are illuminated. (b) and (c) Fluorescence images of a non-fluorescent AN with dispersed fluorescent microtubules. Scale bars, 100 μm.

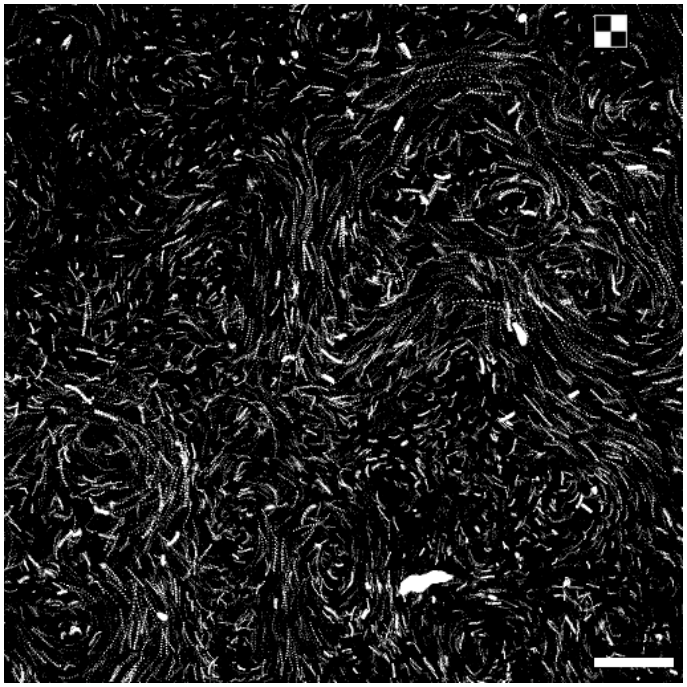

Movie S2. **Activity patterning** Fluorescence images of the active nematic prepared with sparse fluorescent microtubules, indicated for precise PIV measurement. The type of light patterning is indicated in the top righ corner. Scale bar, 100 μm.

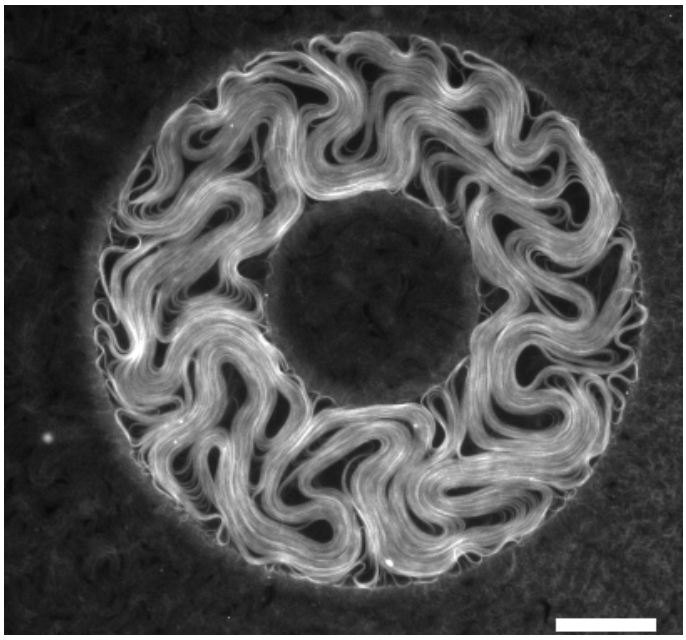

Movie S3. **Ring-shaped channel** Fluorescence images of the active nematic inside a ring-shaped channel. The whole field of view is either illuminated or non-illuminated. Scale bar, 100 μm.

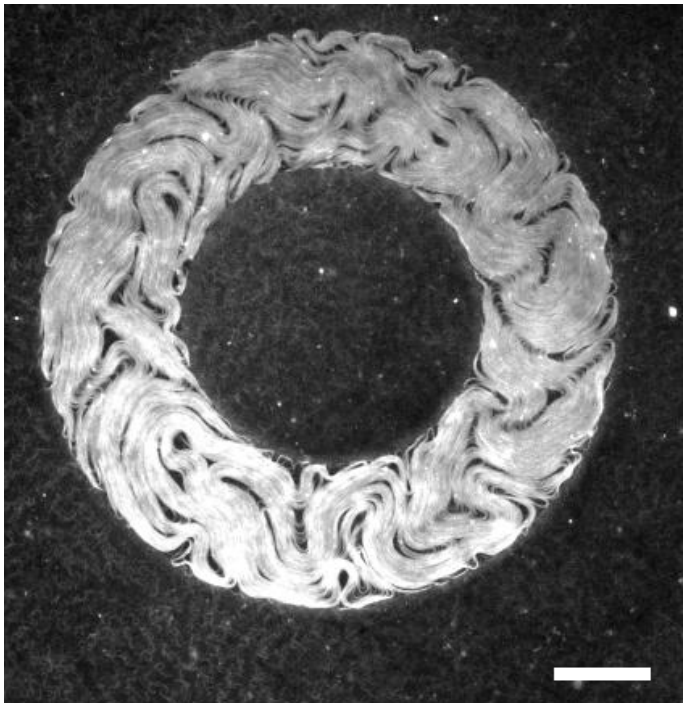

Movie S4. **Ring-shaped channel. Patterned illumination** Fluorescence images of the active nematic inside a ring-shaped channel. Different parts of the field of view are illuminated, as indicated in the top right corner. Scale bar, 100 μm.

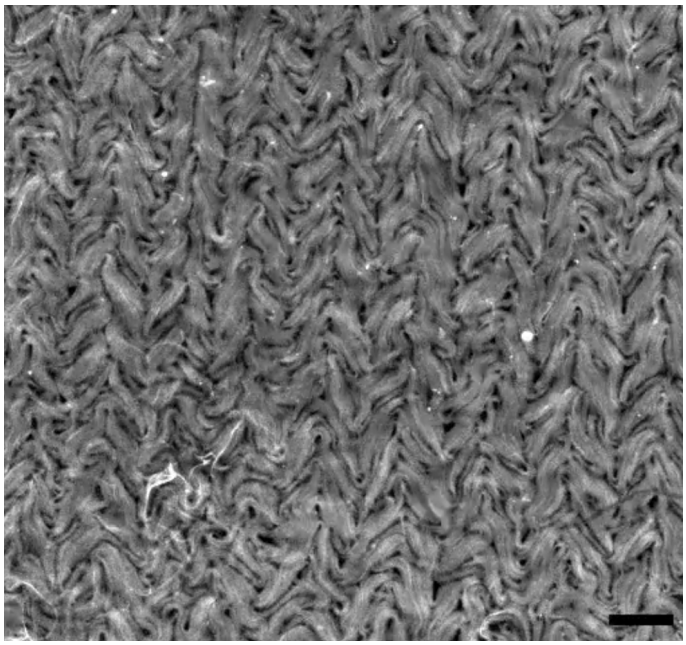

Movie S5. **Alignment transition** Fluorescence images of the active nematic with aligned flows. Different regimes are indicated. Scale bar, 100 μm.